

Received: 2016.03.30  
Accepted: 2016.05.06  
Published: 2016.05.30

# Triptolide Inhibits Invasion and Tumorigenesis of Hepatocellular Carcinoma MHCC-97H Cells Through NF- $\kappa$ B Signaling

Authors' Contribution:  
Study Design A  
Data Collection B  
Statistical Analysis C  
Data Interpretation D  
Manuscript Preparation E  
Literature Search F  
Funds Collection G

AEF 1 **Haiji Wang\***  
DE 2 **Duanye Ma\***  
ACE 1,3 **Chenghong Wang**  
BF 3 **Shanna Zhao**  
AEF 1,4 **Chengbiao Liu**

1 Department of Radiation Oncology, The Affiliated Hospital of Qingdao University, Qingdao, Shandong, P.R. China  
2 Department of Clinical Laboratory, Yuhuangding Hospital, Yantai, Shandong, P.R. China  
3 Department of Clinical Laboratory, Yantaishan Hospital, Yantai, Shandong, P.R. China  
4 Department of General Surgery, Yishui Central Hospital of Linyi, Linyi, Shandong, P.R. China

\* These authors contributed equally to this work

**Corresponding Author:** Shanna Zhao, e-mail: zjpancreas@126.com

**Source of support:** This study was supported by grants from Natural Science Research Foundation of Shandong Province (No: 2014ZRB01198)

**Background:** We investigated whether the plant-derived agent triptolide (TPL) could effectively inhibit the growth and invasion of human hepatocellular carcinoma (HCC) cells.





**Material/Methods:** MHCC-97H cells were treated with various concentration of TPL for various times. To detect the effect of NF- $\kappa$ B on TPL-induced signal pathways, MHCC-97H cells were transfected with p65 siRNA or p65 cDNA, then treated with TPL. We detected cell survival and apoptosis by MTT, soft-agar colony formation assay, flow cytometry, and TUNEL assay. Cell migration and invasion was determined by Matrigel invasion and a wound-healing assay. NF- $\kappa$ B activity was detected by electrophoretic mobility shift assay (EMSA); MMP-9 activity was detected by ELISA. Western blot and real-time PCR (RT-PCR) assays were used to detect p65 and MMP-9 protein and mRNA expression. A subcutaneously implanted tumor model of MHCC-97H cells in nude mice was used to assess the effects of TPL on tumorigenesis *in vivo*.

**Results:** We showed that TPL treatment significantly suppressed growth and induced apoptosis of MHCC-97H cells in a dose- and time-dependent manner *in vitro*. Furthermore, TPL treatment inhibited invasion *in vitro* and inhibited the growth and lung metastasis of MHCC-97H cells *in vivo*. NF- $\kappa$ B and MMP-9 were inactivated with TPL treatment. Overexpression of p65 restored MMP-9 activity and inhibited the TPL anti-tumor effect on MHCC-97H cells. Knockdown of p65 blocked MMP-9 activation and enhanced TPL-induced cell apoptosis and survival inhibition, and TPL inhibition of migration and invasion *in vitro*.

**Conclusions:** TPL treatment inhibited MHCC-97H cell growth, invasion, and metastasis *in vitro* and *in vivo*, suggesting that TPL could be developed as a potential therapeutic agent for the treatment of HCC.

**MeSH Keywords:** **Apoptosis • Carcinoma, Hepatocellular • Medicine, Chinese Traditional**

**Full-text PDF:** <http://www.medscimonit.com/abstract/index/idArt/898801>

 2974   6  32



## Background

Hepatocellular carcinoma (HCC) is the fifth most common malignancy worldwide [1]. Although surveillance of patients with risk factors for HCC and the development of locoregional treatment options have improved outcomes, there are no effective curative methods due to the high invasion, early metastasis, and high tumor recurrence rates of HCC following surgery or interventional treatment [2]. Furthermore, HCC progression, including metastasis, contributes to the high fatality rates of liver cancer. Lymph node metastasis of tumors is considered to be an important factor involved in HCC progression [1].

The transcription factor NF- $\kappa$ B mediates the inducible expression of many genes involved in proliferation, survival, drug resistance, immune and inflammatory responses, angiogenesis and metastasis, and many other biological processes [3,4]. The design of inhibitors which suppress NF- $\kappa$ B activation is therefore of great therapeutic importance in the treatment of HCC. Many studies *in vivo* and *in vitro* have demonstrated that targeting NF- $\kappa$ B signaling could significantly inhibit the growth and metastasis of HCC [5–9]. NF- $\kappa$ B inhibitors also have the potential to inhibit lung metastasis, and pentoxifylline (PTX) is especially promising. Its mechanism of action may involve suppression of VCAM-1 and VEGF-A188 production [10].

Natural products have played significant roles over the years in the development of anticancer drugs. Triptolide (TPL) is a lipophilic extract and the major active compound isolated from *Tripterygium wilfordii* Hook.f., a traditional Chinese medicinal herb that has been used to treat inflammatory diseases for centuries [11]. In addition to immunosuppressive and anti-inflammatory properties, triptolide has attracted extensive research interest for its antitumor effects [12–14]. In hepatocellular carcinoma, TPL was reported to inhibit tumor growth both *in vitro* and *vivo* [15,16], but these studies did not determine whether TPL has an anti-metastasis function. In addition, the mechanisms by which TPL functions in HCC treatment is not clear.

It was recently found that TPL sensitizes glioma-initiating cells to temozolomide by synergistically enhancing apoptosis, which likely results from the augmented repression of NF- $\kappa$ B signaling [17]. In neuroblastoma cells, TPL treatment induced cell death by a mechanism that targets NF- $\kappa$ B signaling [18]. In addition, triptolide has protective effects against organ ischemia/reperfusion injury, the mechanism of which was related to the reduction of NF- $\kappa$ B p65 activity [19–21].

In the present study, we first investigated the role of TPL on growth, apoptosis, invasion, and metastasis of HCC cells *in vitro* and *in vivo*. We then determined the role of NF- $\kappa$ B and its downstream gene MMP-9 on TPL-induced anti-tumor effects.

We found that TPL inhibited NF- $\kappa$ B activity and its downstream MMP-9 gene, which resulted in the inhibition of HCC cell growth, invasion, and metastasis.

## Material and Methods

### Cell lines and culture

The highly metastatic MHCC-97H cell line was purchased from Shanghai Cell Research Institute of the Chinese Academy of Sciences (Shanghai, China). The cells were grown and propagated in RPMI-1640 supplemented with 10% FBS, 2 mmol/L glutamine, 100  $\mu$ g/mL of the antibiotic streptomycin, and 100 U/mL of the antibiotic penicillin. MHCC-97H cells were maintained at 37°C in a 5% CO<sub>2</sub>-humidified atmosphere.

### Triptolide (TPL)

Triptolide (molecular formula, C<sub>20</sub>H<sub>24</sub>O<sub>6</sub>; molecular weight, 360.4 g/mol) was purchased from Santa Cruz Biotechnology, Inc. (Hangzhou, China). Triptolide was dissolved in dimethyl sulfoxide (DMSO). MHCC-97H cells were treated with 1  $\mu$ M, 10  $\mu$ M, and 25  $\mu$ M TPL for 72 hours or 25  $\mu$ M for 2–48 hours.

### Plasmids and transfections

NF- $\kappa$ B p65 siRNA was purchased from Santa Cruz Biotechnology (Santa Cruz, Shanghai, China). Human MHCC-97H cells were transiently transfected with p65 siRNA or with a p65 cDNA plasmid (kindly gifted by Dr. Chen), using Lipofectamine 2000 and following the manufacturer's instruction. After the MHCC-97H cells were transfected with p65 siRNA or p65 cDNA for 6 hours, the cells were exposed to TPL (25 nM) for 48 hours.

### Electrophoretic mobility shift assay (EMSA)

An EMSA assay was used to detect the DNA binding activity of NF- $\kappa$ B according to the manufacturer's instructions. In brief, nuclear proteins were prepared using a nuclear extraction kit and protein concentrations determined by estimation procedures. A biotin-labeled NF- $\kappa$ B probe with a 5'-AGTTGAGGGGACTTTCCAGGC-3' sequence or an unlabeled cold probe was used at 15°C to 20°C for 30 minutes to bind nuclear proteins. Products were separated on a 6% nondenaturing polyacrylamide gel in 0.5 $\times$  tris-borate EDTA buffer at 120 V for 60 minutes at 4°C; the shifted bands corresponding to the protein/DNA complexes were separated relative to the unbound dsDNA. The gel was then transferred onto a presoaked membrane at 300 mA for 30 minutes at 4°C. Following the immobilization of bound oligonucleotides in the membrane by UV-cross-linking for 5 minutes, the shifted bands were visualized after exposure to film.

### Cell viability assay

MHCC-97H cells ( $5 \times 10^3$ ) were seeded in 96-well plates and allowed to adhere for 24 hours. Cells were treated with increasing concentrations (5, 15, or 25  $\mu\text{M}$ ) of triptolide, p65 siRNA, or cDNA for 24–72 hours. Cell viability was determined by a MTT (3-(4,5-dimethylthiazol-2-yl)-2,5-diphenyltetrazolium bromide) assay following the manufacturer's instructions. The results were plotted as mean  $\pm$ SD. All experiments were done in triplicate and repeated at least twice.

### Flow cytometry

After treatment, MHCC-97H cells were collected and fixed overnight at 4°C with 75% ethanol. Propidium iodide staining and flow cytometry analysis was used to evaluate the sub-G1 cell populations for apoptotic rate.

### TUNEL assay

MHCC-97H cells *in vitro* were fixed for 10 minutes with 4% paraformaldehyde. Tissues were dehydrated, embedded, cut into ultrathin sections (5  $\mu\text{m}$ ), and deparaffinized. *In situ* DNA fragmentation was assessed using TUNEL assay on deparaffinized sections, and the number of TUNEL positive cells was determined in three sections per group.

### Matrigel invasion assay

Cell migration and invasion through the Matrigel membrane was quantitated using a commercially available cell invasion kit (Chemicon International, Temecula, CA, USA). Briefly, MHCC-97H cells (already treated with 5 and 25  $\mu\text{M}$  TPL for 24 hours) were harvested with serum-free RPMI 1640 media. Tumor cell suspensions ( $2 \times 10^6$  cells/mL, 100  $\mu\text{L}$ ) were added to the upper compartment of the chamber and incubated for 24 hours. After 24 hours of incubation, the cells in the upper chamber were removed and the cells that had invaded through the Matrigel matrix were stained with 4  $\mu\text{g}/\text{mL}$  calcein AM in Hanks buffered saline at 37°C for 1 hour. The fluorescence of the invaded cells was read at excitation/emission wavelengths of 530/590 nm.

### Wound-healing assay

MHCC-97H cells (already treated with 5 and 25  $\mu\text{M}$  TPL for 24 hours) ( $5 \times 10^4$  cells/well) were seeded into 24-well plates and the cell monolayer was wounded with a 200  $\mu\text{L}$  pipette tip. After washing with PBS three times, 500  $\mu\text{L}$  IMDM media containing 1% FBS was added to the 24-well plates. The remaining cells were cultured in an incubator at 37°C and 5% CO<sub>2</sub>. Cell migration was monitored under a microscope at 100 $\times$  magnification at 0 and 48 hours. Wound closure percentage=(1-wound area at a certain time point)/starting wound area.

### MMP-9 activity assay

MHCC-97H cells were treated with 5 and 25  $\mu\text{M}$  TPL for 48 hours. Levels of MMP-9 (matrix metalloproteinase 9) in the cell culture media were measured with a human MMP-9 activity assay kit (Guangzhou, China) according to the manufacturer's instructions.

### Western blot analysis

MHCC-97H cells in different groups were lysed and the protein was extracted. The protein concentration was determined using the Bio-Rad assay system (Bio-Rad, Hercules, CA). For immunoblotting, proteins were separated by SDS/PAGE and transferred to a nitrocellulose membrane, then incubated with p65 and MMP-9 specific antibodies. Immune complexes were detected with a sheep anti-mouse immunoglobulin antibody conjugated to horseradish peroxidase, and visualized using enhanced chemiluminescence reagent (Amersham) according to the manufacturer's instructions.

### Real-time PCR (RT-PCR)

MHCC-97H cells were seeded in 6-well plate and treated with 5 and 25  $\mu\text{M}$  TPL for 48 hours. Total RNA was isolated using the RNeasy Mini Kit (Qiagen, Shanghai, China) according to the manufacturer's protocol, and cDNA was generated using the ThermoScript™ RT-PCR System for RT-PCR (Invitrogen Life Technologies, Carlsbad, CA and Shanghai, China), according to the manufacturer's protocol. The gene-specific primers are listed below:

p65: 5'-GCG AGA GGA GCA CAG ATA CC-3' and 5'-CTG ATA GCC TGC TCC AGG TC-3'; MMP-9: 5'-TACCACCTCGAAGCTTTGACAGCGA-3' and 5'-AAAGGCACAGTAGTGGCCGTAGAA-3'. The primers for  $\beta$ -actin, a control gene, were: 5'-TGTTGGCATCAATGACCCCTT-3' and 5'-CTCCAGACGACTACTAGCG-3'. Thermocycling was 94°C for 40 seconds, 60°C for 40 seconds (30 cycles), and 72°C for 5 minutes. The expression level was calculated by dividing the integrated band intensity of the experimental samples by that of the control sample.

### Mouse xenograft growth and lung metastasis assay

The Ethics Committee of the Yishui Central Hospital of Linyi approved the protocols for animal care and handling in this study. Four-week-old female BALB/c (nu/nu) mice were obtained from the Animal Research Center of the Shandong University (Jinan, China). MHCC-97H cells ( $1 \times 10^7$ ) in 200  $\mu\text{L}$  of a suspension mixture with Matrigel (BD Biosciences) were subcutaneously inoculated into the left flank of mice. When tumor volume reached 80 to 100 mm<sup>3</sup> (about 4 weeks), mice were divided randomly into 3 groups, (six mice per group): 1)

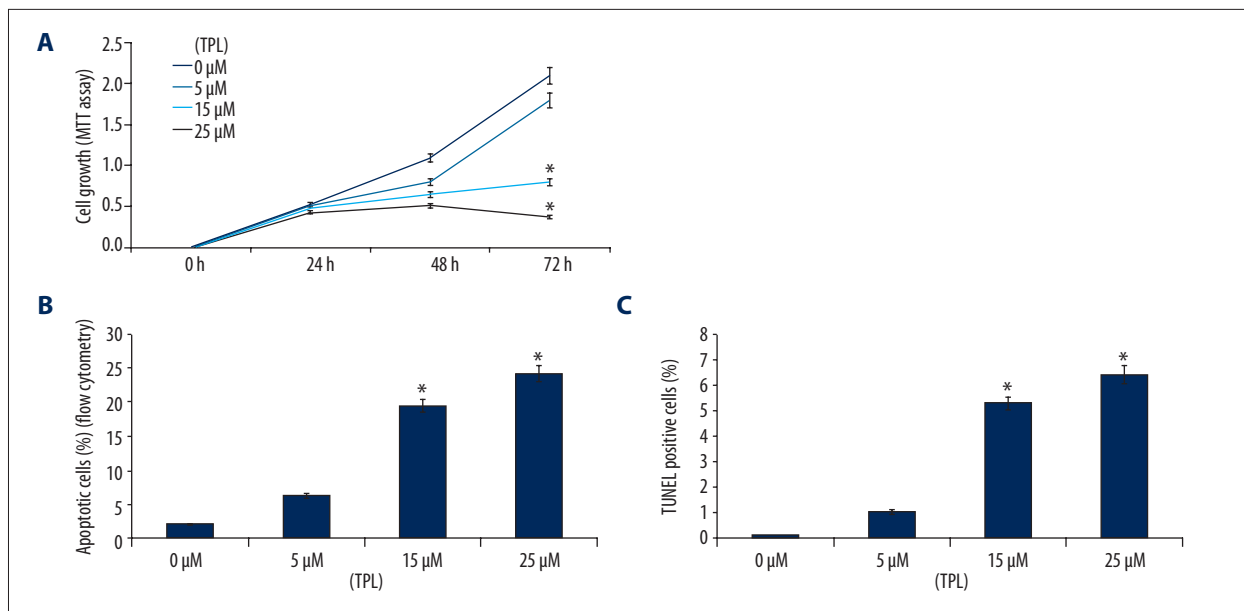


**Figure 1.** Effect of TPL on MHCC-97H cell growth and apoptosis. **(A)** Dose and time responses of growth of MHCC-97H cells with TPL treatment. Cells were seeded in 96-well plates at 5,000 cells per well and treated with varied concentrations of TPL or for different time periods. After treatment, cell densities were determined by MTT assay. Each value represents the mean  $\pm$ SD (n=5) of 3 independent experiments. \*  $p < 0.05$ , compared to the control. **(B)** Cell death assay for measuring apoptosis induced by TPL. Apoptosis was measured by flow cytometry. Values are reported as mean  $\pm$ SD. \*  $p < 0.05$ , compared to the control. Cell apoptosis was also detected by TUNEL assay. Values are reported as mean  $\pm$ SD. \*  $p < 0.05$ , compared to the control.

mice injected with MHCC-97H cells and treated with TPL; 2) mice injected with MHCC-97H cells and treated with vehicle; and 3) mice receiving no cells but treated with TPL to assess toxicity. In group 1, mice were injected with TPL at 0.4 mg/kg daily for 15 days; in group 2, mice were injected with vehicle (DMSO); in group 3, mice were injected with TPL at 0.4 mg/kg daily for 15 days. Tumor volume (length $\times$ width $\times$ depth $\times$ 0.52) was measured once a week. Body weights were recorded every week. Xenograft tumors were frozen in liquid nitrogen or fixed in 10% formalin and embedded in paraffin. NF- $\kappa$ B and MMP-9 activity and expression, NF- $\kappa$ B p65 expression, and apoptosis were detected. The lungs of the mice were fixed, paraffin embedded, cut, and stained with hematoxylin and eosin (H&E). The number of metastatic nodes on the lung surface was counted.

### Statistical analysis

The significance of the difference between the control and each experimental group was analyzed by Student's t-test (two-tailed). Values are expressed as the mean  $\pm$ SE from at least three separate experiments and differences were considered significant at  $p < 0.05$ .

## Results

### TPL-induced cell growth inhibition and apoptosis of MHCC-97H cells

MHCC-97H cells were treated with 5, 15, or 25  $\mu$ M TPL for 24–72 hours. As shown in Figure 1A, TPL treatment resulted in cell growth inhibition in a dose- and time-dependent manner in MHCC-97H cells by MTT assay. The induction of apoptosis by TPL in MHCC-97H cells was also found in a dose-dependent manner by flow cytometry assay (Figure 1B) and TUNEL assay (Figure 1C). These results provided convincing data that TPL induced apoptosis, resulting in cell growth inhibition in MHCC-97H cells.

### TPL inhibits NF- $\kappa$ B activation

Since NF- $\kappa$ B has been shown to be involved in apoptosis and cell survival, we wanted to see whether TPL-induced apoptosis in MHCC-97H is mediated by modulation of the NF- $\kappa$ B pathway. In order to reveal the molecular mechanism of TPL, we first determined the concentration-dependent effect of TPL on NF- $\kappa$ B activity and phosphorylation of p65 in MHCC-97H cells. MHCC-97H cells treated with 5, 15, or 25  $\mu$ M TPL for 72 hours resulted in a significant dose-dependent decrease in NF- $\kappa$ B activity. NF- $\kappa$ B DNA binding was measured by EMSA (Figure 2A) and phosphorylation of p65 by western blot assay (Figure 2C). Similarly, when treated with 25  $\mu$ M TPL for 24–72

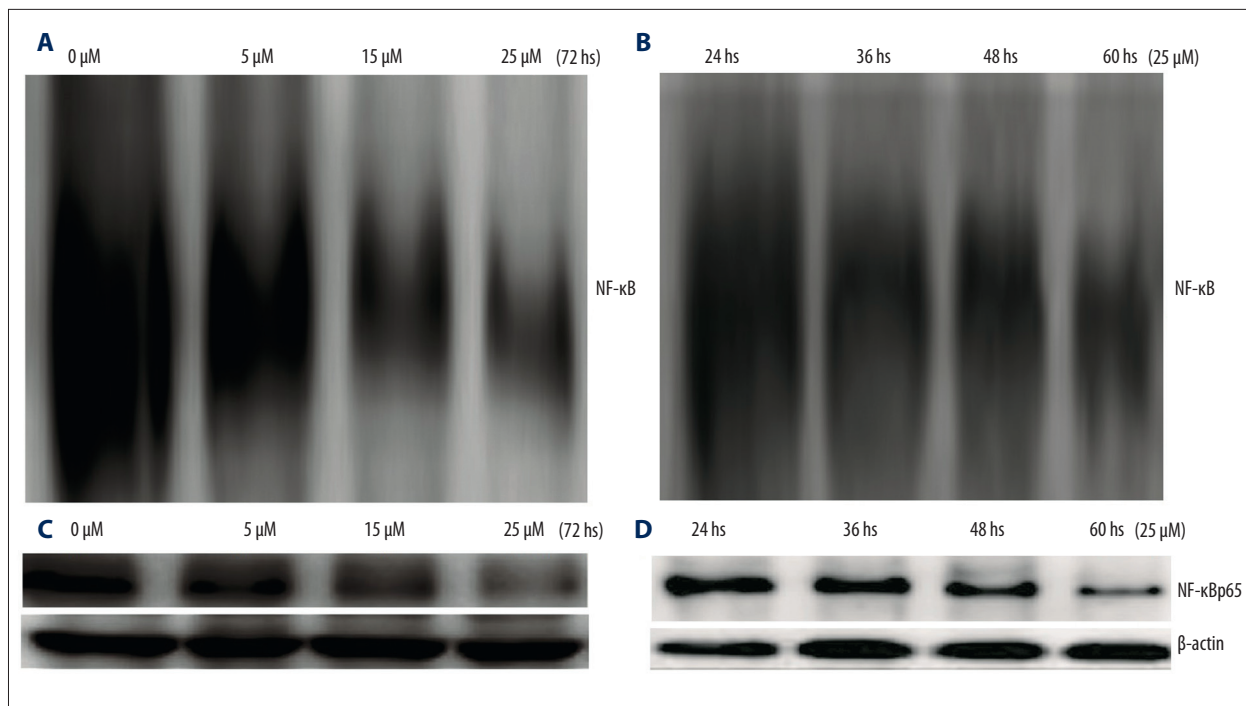


**Figure 2.** Effect of TPL on NF- $\kappa$ B activity and NF- $\kappa$ B p65 expression in MHCC-97H cell. **(A)** MHCC-97H cells were treated with 5, 15, or 25  $\mu$ M TPL for 72 hours. Nuclear extracts were prepared from control and treated cells and subjected to analysis for NF- $\kappa$ B DNA-binding activity as measured by EMSA. **(B)** MHCC-97H cells were treated with 25  $\mu$ M TPL for 24–60 hours. Nuclear extracts were prepared from control and treated cells and subjected to analysis for NF- $\kappa$ B DNA-binding activity as measured by EMSA. **(C)** MHCC-97H cells were treated with 5, 15, or 25  $\mu$ M TPL for 72 hours. NF- $\kappa$ B p65 protein was detected by western blot assay; **(D)** MHCC-97H cells were treated with 25  $\mu$ M TPL for 24–60 hours. NF- $\kappa$ B p65 protein was detected by western blot assay.

hours, we observed a significant time-dependent decrease in NF- $\kappa$ B activity and phosphorylation of p65 measured by EMSA (Figure 2B) and western blot assay (Figure 2D).

### TPL induces apoptosis by inhibition of NF- $\kappa$ B activity

Since our results showed a significant decrease in NF- $\kappa$ B activity by TPL treatment, we next questioned whether this change could affect apoptosis and growth of MHCC-97H cells. We transfected NF- $\kappa$ B p65 cDNA or siRNA into MHCC-97H cells, treated the transfected cells with TPL, and detected NF- $\kappa$ B activity and TPL-induced apoptosis. As shown in Figure 3A, p65 cDNA transfection caused a significant increase in the TPL-induced NF- $\kappa$ B activity. We further evaluated the effect of p65 overexpression on TPL-induced apoptosis, and observed a significant decrease in TPL-induced apoptosis (Figure 3B, 3C). In contrast, knockdown of p65 by p65 siRNA transfection caused a significant decrease in TPL-induced NF- $\kappa$ B activity (Figure 3D). We further evaluated the effect of p65 silencing on TPL-induced apoptosis, and observed a significant increase in TPL-induced apoptosis (Figure 3E, 3F). These results demonstrated that TPL-induced apoptosis of MHCC-97H cells was mediated by NF- $\kappa$ B inactivity.

### MMP-9 activity and expression by TPL is regulated by NF- $\kappa$ B

We then tested the effect of TPL on MMP-9 activity, MMP-9 mRNA, and MMP-9 protein expression. MHCC-97H cells treated with 15 or 25  $\mu$ M TPL for 48 hours dramatically decreased MMP-9 mRNA and MMP-9 protein expression in a dose-dependent manner (Figure 4A, 4B). TPL treatments lead to about a 2.4-fold decrease in MMP-9 activity when treated with 15  $\mu$ M TPL for 48 hours, and a 3.6-fold decrease in MMP-9 activity when treated with 25  $\mu$ M TPL for 48 hours (Figure 4C). However, p65 cDNA transfection increased TPL-induced MMP-9 expression and activity (data not shown). These results are in line with the previous observation that knockdown of NF- $\kappa$ B activity blocked MMP-9 expression and MMP-9 activation [22,23].

### TPL inhibits migration and invasion of MHCC-97H cells

The effects of TPL on MHCC-97H cell invasion and migration were analyzed by a wound-healing assay and by Transwell Boyden chamber assay. In the wound-healing assay, the results showed that the area change for wound-healing in the TPL treated MHCC-97H cells was reduced compared to the



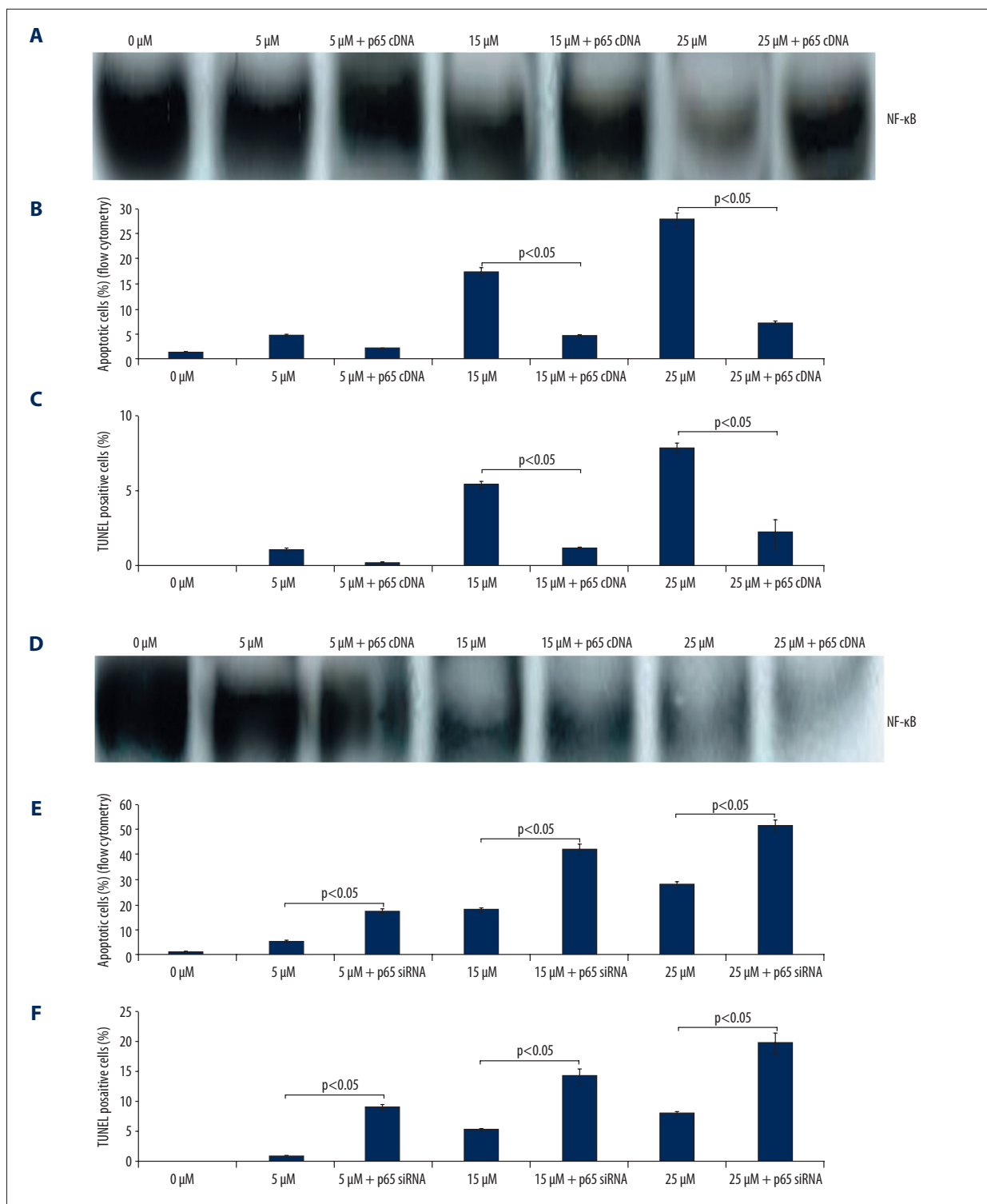


**Figure 3.** TPL induces apoptosis by inhibition of NF-κB activity. **(A)** The effect of p65 cDNA transfection and TPL treatment on NF-κB DNA-binding activity by EMSA assay. **(B)** Induction of apoptosis by p65 cDNA and TPL in MHCC-97H cells tested by flow cytometry. **(C)** Induction of apoptosis by p65 cDNA and TPL in MHCC-97H cells tested by TUNEL assay. **(D)** the effect of p65 siRNA transfection and TPL on NF-κB DNA-binding activity by EMSA assay. **(E)** Induction of apoptosis by p65 siRNA and TPL in MHCC-97H cells tested by flow cytometry. **(F)** Induction of apoptosis by p65 siRNA and TPL in MHCC-97H cells tested by TUNEL assay. Values are reported as mean ±SD.  $p < 0.05$ , compared to the control.

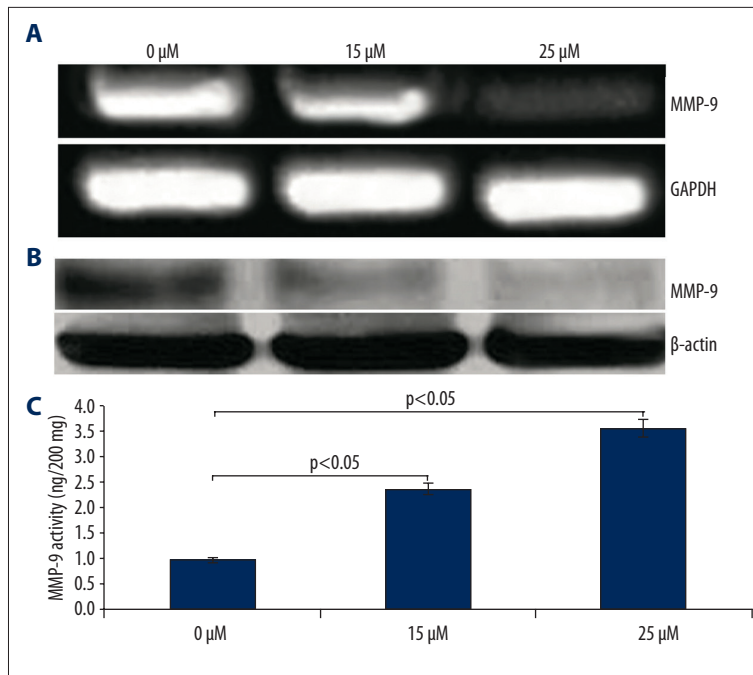


**Figure 4.** Effect of TPL on MMP-9 gene transcription, expression, and its activity. MHCC-97H cells were treated with 15 and 25  $\mu$ M TPL for 72 hours. **(A)** TPL inhibits the MMP-9 mRNA expression, measured by real-time PCR (RT-PCR) analysis. **(B)** TPL inhibits MMP-9 protein expression, measured by western blot analysis. **(C)** TPL inhibits MMP-9 activity vs. control, measured by ELISA assay, *p* < 0.05.

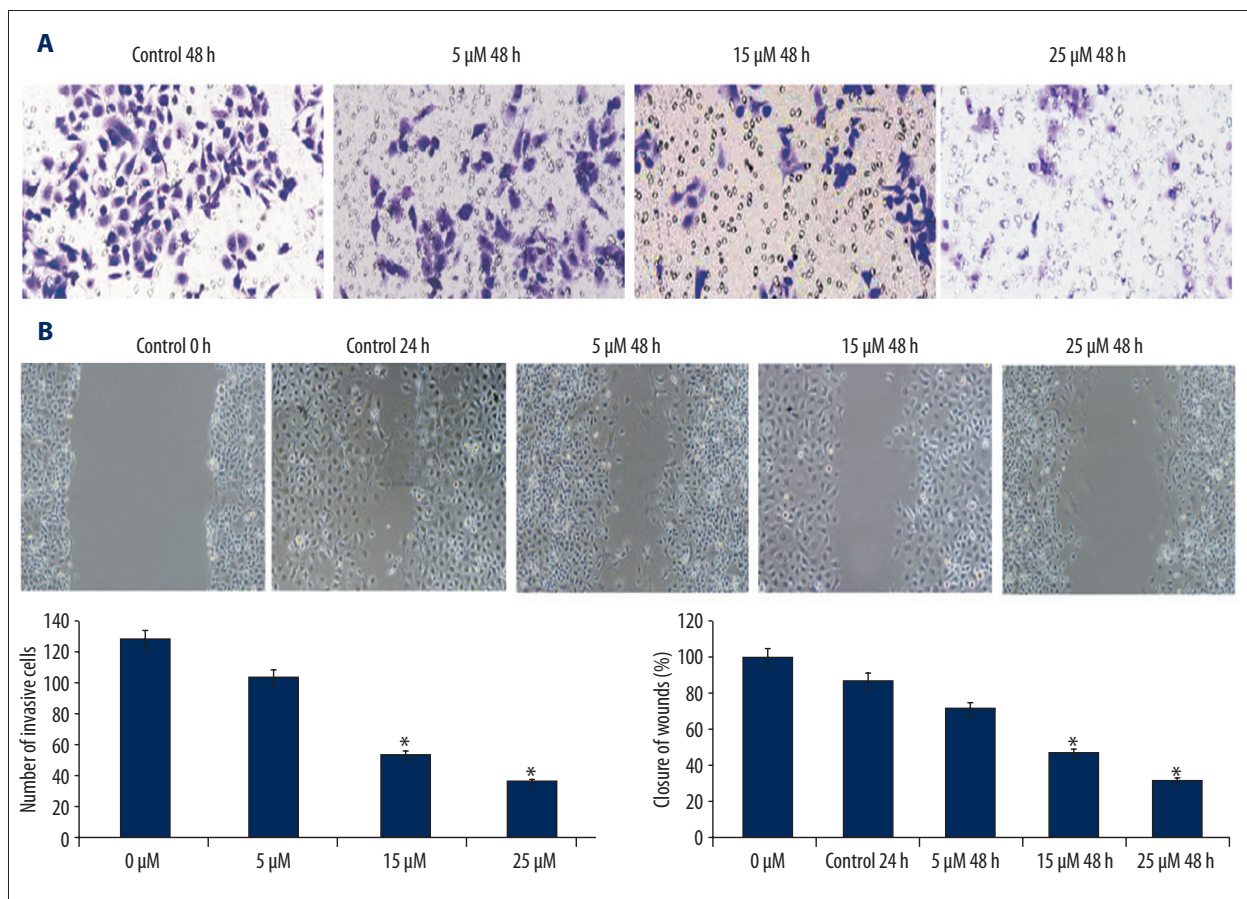


**Figure 5.** TPL inhibits migration and invasion of MHCC-97H cells. **(A)** Cell migratory ability detected by Transwell migration assay. **(B)** Cell migratory ability detected by wound healing assay. Data is presented as the mean  $\pm$ SD; *p* values were calculated with the Student's *t*-test. \* *p* < 0.05

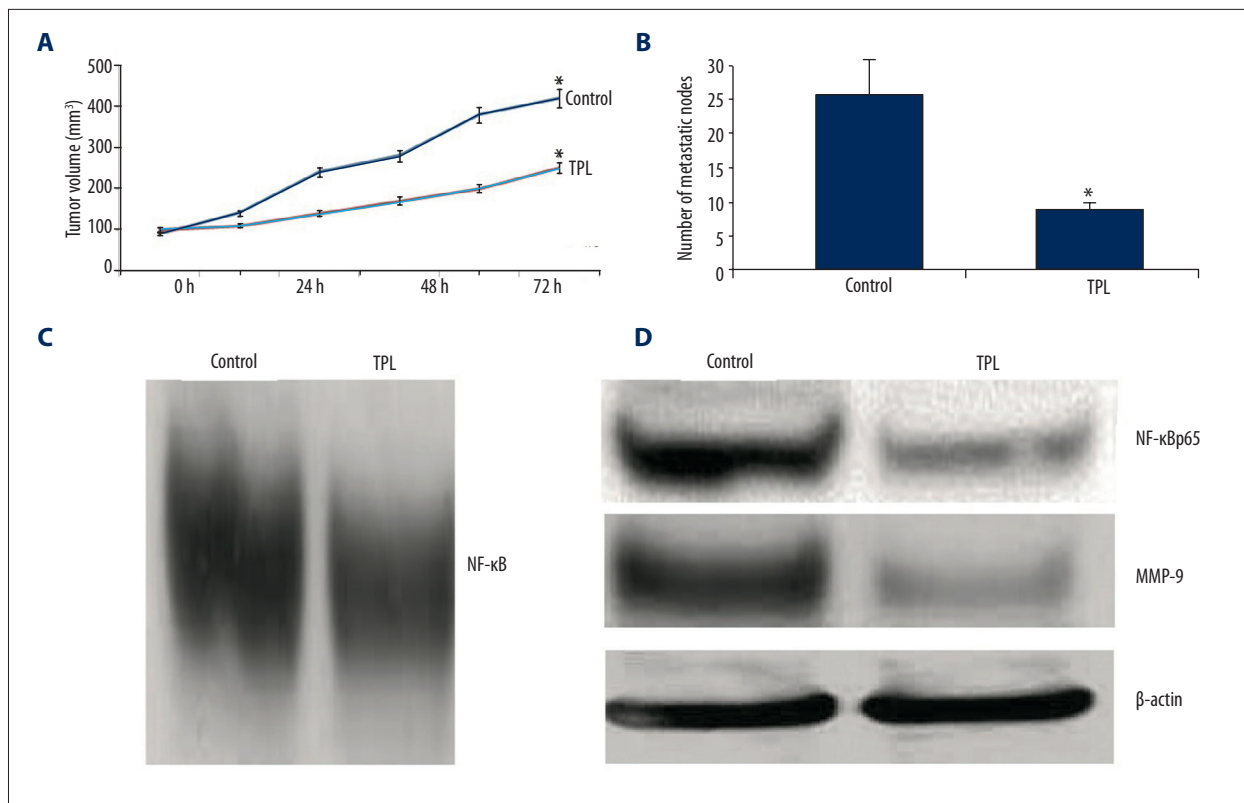


**Figure 6.** TPL inhibits tumor growth and the expression of NF- $\kappa$ B target genes *in vivo*. MHCC-97H xenografts were generated by inoculating cells subcutaneously (s.c.) in SCID mice. Once transplanted, the cells developed into palpable tumors (about 80 mg), and groups of 10 animals were classified randomly and assigned to different treatment groups. Mice were injected with TPL at 0.4 mg/kg daily for 15 days. The control group received vehicle only. **(A)** TPL retards the growth of MHCC-97H tumor xenografts in nude mice. Tumor volumes in SCID mice were plotted against time; \*  $p < 0.05$ , compared to the control. **(B)** The number of metastatic nodes in each group. Lung tumors were counted with the naked eye. The data represent the mean and the standard deviation ( $n = 10$ ).  $p$  values were calculated with the Student's  $t$ -test. \*  $p < 0.05$ . Black is a metastatic node. **(C)** TPL inhibits NF- $\kappa$ B DNA-binding activity *in vivo*. Tumor xenografts were removed, and nuclear protein extracts were prepared. Binding of NF- $\kappa$ B consensus elements with nuclear extracts was detected by EMSA. **(D)** The expression of NF- $\kappa$ B p65 and MMP-9 was detected by western blotting of tumor tissue extracts. TPL inhibited the expression of NF- $\kappa$ B p65 and MMP-9 in tumor tissues of TPL treated animals compared to controls.

vehicle-treated cells ( $p < 0.05$ ) (Figure 5A). In the Transwell Matrigel invasion assays, the results showed that the number of cells in the lower chamber of the Transwell was significantly decreased in TPL treated MHCC-97H cells compared to the vehicle-treated cells ( $p < 0.05$ ) (Figures 5B). Taken together, these results indicated that TPL inhibits both the migration and invasion of MHCC-97H cells.

#### Effect of TPL on growth and lung metastasis of MHCC-97H cells *in vivo*

The inhibitory effect of TPL on MHCC-97H cell growth and lung metastasis was confirmed in an *in vivo* xenograft mouse model. As shown in Figure 6A, TPL treatment significantly inhibited tumor growth compared to untreated control ( $p < 0.05$  vs. control). In addition, fewer metastatic nodes were formed on the surface of lungs in the TPL treated groups than the control

group (Figure 6B,  $p < 0.05$  vs. control). TPL treatment did not cause significant changes in animal body weight (data not shown). Western blot analysis of xenograft tumors showed that the expression of p65 and MMP-9 were markedly decreased in TPL-treated tumors compared to vehicle-treated tumors (Figure 6D). EMSA assay showed that NF- $\kappa$ B activity was also markedly decreased in TPL-treated tumors compared to vehicle-treated tumors (Figure 6C).

#### Discussion

Triptolide is a small diterpenoid triepoxide, originally purified from the Chinese medicinal herb *Tripterygium wilfordii* Hook.f. Besides anti-inflammatory and immunosuppressive effects, triptolide has been demonstrated to inhibit proliferation and induce apoptosis of cancer cells *in vitro* and inhibit the growth



and metastasis of tumors *in vivo* [23–25]. However, the mechanism of action of triptolide on tumor growth and invasion still remained unclear.

The present study was designed to investigate the mechanism by which TPL inhibited the NF- $\kappa$ B activation pathway, which has been closely linked to tumor cell survival, proliferation, invasion, and metastasis. Our results demonstrated that TPL at concentrations between 5 and 25  $\mu$ M inhibited cell growth and induced apoptosis of MHCC-97H cells in a dose- and time-dependent manner. In addition, TPL suppressed invasion *in vitro* and lung metastasis and tumor growth in a nude mouse model.

Numerous studies have reported that the NF- $\kappa$ B pathway is associated with survival, apoptosis, and metastasis of many cancer cell types, including HCC cells [5–9,26,27]. The antitumor effect induced by TPL has been reported to be associated with the down-regulation of NF- $\kappa$ B activity [28–30]. In the present study, we found that TPL inhibited NF- $\kappa$ B activity and p65 expression in a dose- and time-dependent manner. To further investigate whether the effect of TPL on growth and apoptosis of MHCC-97H cells was mediated through the NF- $\kappa$ B pathway, we first transfected p65 cDNA plasmid into the MHCC-97H cells, and found that p65 cDNA transfection induced NF- $\kappa$ B activation. However, TPL treatment abrogated the activation of NF- $\kappa$ B induced by the p65 cDNA transfection. The TPL-induced apoptosis of MHCC-97H cells was also inhibited by the p65 cDNA transfection. We next transfected a p65 siRNA plasmid into the MHCC-97H cells, and found that p65 siRNA knockdown exerted an inhibitory effect on NF- $\kappa$ B activation. Furthermore, p65 knockdown increased TPL-induced apoptosis and growth inhibition of MHCC-97H cells. Thus, our results clearly showed that TPL inhibits proliferation and induces apoptosis of MHCC-97H cells by inhibition of NF- $\kappa$ B signaling.

## References:

1. Parkin DM, Bray F, Ferlay J, Pisani P: Global cancer statistics, 2002. *Cancer J Clin*, 2005; 55: 74–108
2. El-Serag HB: Hepatocellular carcinoma: An epidemiologic view. *J Clin Gastroenterol*, 2002; 35: 572–78
3. Chan CF1, Yau TO, Jin DY et al: Evaluation of nuclear factor-kappa B, urokinase-type plasminogen activator, and HBx and their clinicopathological significance in hepatocellular carcinoma. *Clin Cancer Res*, 2004; 10: 4140–49
4. Wang F, Yang JL, Yu KK et al: Activation of the NF- $\kappa$ B pathway as a mechanism of alcohol enhanced progression and metastasis of human hepatocellular carcinoma. *Mol Cancer*, 2015; 14: 10
5. Chiang IT, Liu YC, Wang WH et al: Sorafenib inhibits TPA-induced MMP-9 and VEGF expression via suppression of ERK/NF- $\kappa$ B pathway in hepatocellular carcinoma cells. *In vivo*, 2012; 26: 671–81
6. Xing S, Zhang B, Hua R et al: URG4/URGCP enhances the angiogenic capacity of human hepatocellular carcinoma cells *in vitro* via activation of the NF- $\kappa$ B signaling pathway. *BMC Cancer*, 2015; 15: 368
7. Neelgundmath M, Dinesh KR, Mohan CD et al: Novel synthetic coumarins that targets NF- $\kappa$ B in hepatocellular carcinoma. *Bioorg Med Chem Lett*, 2015; 25: 893–97
8. Cui Y, Lin C, Wu Z et al: AGK enhances angiogenesis and inhibits apoptosis via activation of the NF- $\kappa$ B signaling pathway in hepatocellular carcinoma. *Oncotarget*, 2014; 5: 12057–69
9. Zhang N, Chu ES, Zhang J et al: Peroxisome proliferator activated receptor alpha inhibits hepatocarcinogenesis through mediating NF- $\kappa$ B signaling pathway. *Oncotarget*, 2014; 5: 8330–40
10. Futakuchi M, Ogawa K, Tamano S et al: Suppression of metastasis by nuclear factor kappaB inhibitors in an *in vivo* lung metastasis model of chemically induced hepatocellular carcinoma. *Cancer Sci*, 2004; 95: 18–24
11. Brinker AM, Ma J, Lipsky PE, Raskin I: Medicinal chemistry and pharmacology of genus tripterygium (celastraceae). *Phytochemistry*, 2007; 68: 732–66
12. Jiang QW, Cheng KJ, Mei XL et al: Synergistic anticancer effects of triptolide and celastrol, two main compounds from thunder god vine. *Oncotarget*, 2015; 6: 32790–804
13. Reno TA, Kim JY, Raz DJ: Triptolide inhibits lung cancer cell migration, invasion, and metastasis. *Ann Thorac Surg*, 2015; 100: 1817–24
14. Jacobson BA, Chen EZ, Tang S et al: Triptolide and its prodrug minnelide suppress Hsp70 and inhibit *in vivo* growth in a xenograft model of mesothelioma. *Genes Cancer*, 2015; 6: 144–52
15. Alsaied OA, Sangwan V, Banerjee S et al: Sorafenib and triptolide as combination therapy for hepatocellular carcinoma. *Surgery*, 2014; 156: 270–79

It has been reported that NF- $\kappa$ B is involved in MMP-9 up-regulation, which is crucial for regulating cell invasion and metastasis in different cell types [31,32]. In this study, we showed that TPL inhibited NF- $\kappa$ B activity and down-regulated MMP-9 gene expression and MMP-9 activity in MHCC-97H cells. Furthermore, p65 cDNA transfection increased TPL-induced MMP-9 activation, suggesting that MMP-9 was regulated by NF- $\kappa$ B signaling. Since we observed that TPL inhibited the expression and activity of MMP-9, we tested the effects of TPL on the migration and invasion of MHCC-97H cells. Our results demonstrated that tumor cell invasion *in vitro*, which is normally mediated through MMP-9, is suppressed by TPL.

We next tested the effect of TPL on MHCC-97H cells in a mouse xenograft model. Our results showed that TPL was effective in inhibiting tumor growth and lung metastasis, the results of which were consistent with inactivation of NF- $\kappa$ B and MMP-9. Thus, overall our results provide a novel mechanistic insight into the ability of TPL to block NF- $\kappa$ B/MMP-9 activation, resulting in reduced invasion and tumor growth inhibition of MHCC-97H cells.

## Conclusions

Our study provides evidence that TPL inhibits tumor growth, invasion, and lung metastasis in MHCC-97H cells both *in vitro* and *in vivo*. TPL may provide a novel agent for treatment of HCC. The results presented here provide the basis for the initial animal studies required for clinical trials with this agent.

## Conflicts of interest

No potential conflicts of interest were disclosed.

16. Ling D, Xia H, Park W et al: pH-sensitive nanoformulated triptolide as a targeted therapeutic strategy for hepatocellular carcinoma. *ACS Nano*, 2014; 8: 8027–39
17. Sai K, Li WY, Chen YS et al: Triptolide synergistically enhances temozolomide-induced apoptosis and potentiates inhibition of NF- $\kappa$ B signaling in glioma initiating cells. *Am J Chin Med*, 2014; 42: 485–503
18. Krosch TC, Sangwan V, Banerjee S et al: Triptolide-mediated cell death in neuroblastoma occurs by both apoptosis and autophagy pathways and results in inhibition of nuclear factor-kappa B activity. *Am J Surg*, 2013; 205: 387–96
19. Wu C, Wang P, Rao J et al: Triptolide alleviates hepatic ischemia/reperfusion injury by attenuating oxidative stress and inhibiting NF- $\kappa$ B activity in mice. *J Surg Res*, 2011; 166: e205–13
20. Hao M, Li X, Feng J, Pan N: Triptolide protects against ischemic stroke in rats. *Inflammation*, 2015; 38: 1617–23
21. Bai S, Hu Z, Yang Y et al: Anti-inflammatory and neuroprotective effects of triptolide via the NF- $\kappa$ B signaling pathway in a rat MCAO model. *Anat Rec*, 2016; 299: 256–66
22. Lee SU, Ahn KS, Sung MH et al: Indacaterol inhibits tumor cell invasiveness and MMP-9 expression by suppressing IKK/NF- $\kappa$ B activation. *Mol Cells*, 2014; 37: 585–91
23. Li C, Guo S, Shi T: Role of NF- $\kappa$ B activation in matrix metalloproteinase 9, vascular endothelial growth factor and interleukin 8 expression and secretion in human breast cancer cells. *Cell Biochem Funct*, 2013; 31: 263–68
24. Phillips PA, Dudeja V, McCarroll JA et al: Triptolide induces pancreatic cancer cell death via inhibition of heat shock protein 70. *Cancer Res*, 2007; 67: 9407–16
25. Zhu W, Ou Y, Li Y et al: A small-molecule triptolide suppresses angiogenesis and invasion of human anaplastic thyroid carcinoma cells via downregulation of the nuclear factor-kappa B pathway. *Mol Pharmacol*, 2009; 75: 812–19
26. Bauerle KT, Schweppe RE, Haugen NR: Inhibition of nuclear factor-kappa B differentially affects thyroid cancer cell growth, apoptosis, and invasion. *Mol Cancer*, 2010; 9: 117
27. Pacak K, Sirova M, Giubellino A et al: NF- $\kappa$ B inhibition significantly upregulates the norepinephrine transporter system, causes apoptosis in pheochromocytoma cell lines and prevents metastasis in an animal model. *Int J Cancer*, 2012; 131: 2445–55
28. Ou CC, Chen YW, Hsu SC et al: Triptolide inhibits the proliferation of cells from lymphocytic leukemic cell lines in association with downregulation of NF- $\kappa$ B activity and miR-16-1. *Evid Based Complement Alternat Med*, 2012; 2012: 350239
29. Meng HT, Zhu L, Ni WM et al: Triptolide transcriptionally represses HER2 in ovarian cancer cells by targeting NF- $\kappa$ B. *Acta Pharmacol Sin*, 2011; 32: 503–11
30. Liu L, Salnikov AV, Bauer N et al: Triptolide reverses hypoxia-induced epithelial-mesenchymal transition and stem-like features in pancreatic cancer by NF- $\kappa$ B downregulation. *Int J Cancer*, 2014; 134: 2489–503
31. Rosenberg GA: Matrix metalloproteinases in neuroinflammation. *Glia*, 2002; 39: 279–91
32. Ditsworth D, Zong WX: NF- $\kappa$ B: Key mediator of inflammation-associated cancer. *Cancer Biol Ther*, 2004; 3: 1214–16